JOURNAL OF APPLIED ELECTROCHEMISTRY **14** (1984) 323–327

Electrochromic properties of the n-heptyl viologen–ferrocyanide system

A. YASUDA, H. MORI, Y. TAKEHANA, A. OHKOSHI

Sony Corporation, Electronic Devices Division, Development Centre, 7–35 Kitashinagawa 6-chome, Shinagawa-ku, Tokyo 141, Japan

N. KAMIYA

Research Institute for Energy Materials, Yokohama National University, 156 Tokiwadai, Hodogaya, Yokohama 240, Japan

Received 4 May 1983; revised 16 August 1983

Electrochromic properties of the mixed solution of n-heptyl viologen dibromide (HV), $Fe(CN)_6^{4-}$ and NaH_2PO_2 or KBr were investigated by cyclic voltammetry and the transparency–time relation. When $Fe(CN)_6^{4-}$ is added to a HV solution the mixture colours violet without inputting any voltage. However, the colour fades gradually by further addition of NaH_2PO_2, and the transparency of the mixture increases with addition of larger amounts of NaH_2PO_2. The same effect was observed by addition of KBr to the HV–$Fe(CN)_6^{4-}$ solution. The input voltage required for the electrochromism of HV is lowered considerably by addition of $Fe(CN)_6^{4-}$, when NaH_2PO_2 or KBr plays a role in controlling the colouring–erasing phenomena. The HV–$Fe(CN)_6^{4-}$–KBr system showed some HV 'residue' in the cyclic voltammogram on an indium–tin oxide (ITO) electrode, while no such HV 'residue' was observed in the HV–$Fe(CN)_6^{4-}$–NaH_2PO_2 system. The HV–$Fe(CN)_6^{4-}$–NaH_2PO_2 system is superior in colouring–erasing reproducibility and in response time to the HV solution or the HV–$Fe(CN)_6^{4-}$ system.

---

1. Introduction

During the past decade, concentrated studies have been made on application of the viologen redox reaction,

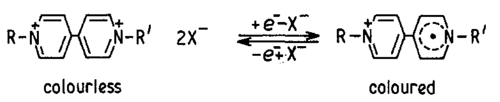

(1)

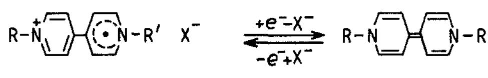

(2)

to electrochromic display (ECD) [1–6]. Nevertheless the viologen ECD has not yet become available for display devices because of its low reliability and slow speed of response. Another problem in the development of viologen ECD is that repetitions of redox cycles of viologen cause 'residue' on the electrode. Ponjeé *et al.* [1] reported that tetramethylene bis-4(1-ethylpyridin-4-yl) pyridinium perchlorate has the effect of improving the 'residue' problem, while Barna *et al.* [2] showed that the 'residue' on the electrode is caused by intermolecular interaction between adjacent viologen molecules, and asymmetric viologen molecules with at least one bulky end group would decrease intermolecular stacking and, in consequence, improve the redox cycles in number.

On the other hand, an attempt was made by us to add $K_4Fe(CN)_6$ in order to decrease the applied voltage. If the applied voltage were lowered, viologen would be prevented from decomposition and the electrodes would also be prevented from degradation.

From the standpoint of the standard redox potentials of $Fe(CN)_6^{3-}/Fe(CN)_6^{4-}$ and n-heptyl viologen dibromide (HV, $R = R' = C_7H_{15}$ and $X = Br$ in Equation 1), $Fe(CN)_6^{4-}$ would never reduce HV, however, the HV–$Fe(CN)_6^{4-}$ mixed solution colours without any input of voltage and, furthermore, some yellow residue appears on the electrode in the anodic scan. Addition of NaH_2PO_2

0021-891X/84 $03.00 + .12

or KBr to the mixture was found to make the HV–$Fe(CN)_6^{4-}$ solution nearly transparent, leading to an increase in the contrast ratio, and the appropriate addition of NaH_2PO_2 also contributed to the improvement of both the problem of the viologen 'residue' and the response time.

2. Experimental details

2.1. *Potential sweep voltammetry*

n-Heptyl viologen dibromide was supplied by the Japanese Research Institute for Photosensitizing Dyes Co. Ltd and was used without further purification.

Cyclic voltammograms were taken using a Hokuto Denko HA301 potentiostat and a HB104 function generator. A Pt wire 1.7 cm long and of diameter 0.65 mm or an indium–tin oxide (ITO) transparent glass electrode (effective area of 0.95 cm^2) was used as the working electrode.

All solutions were deoxygenated by passing nitrogen through them.

2.2. *ITO glass cell for spectrophotometry*

An ITO glass cell (Fig. 1) was set in the sample beam position of a Hitachi 220A double beam monochrometer, which monitored the change of the absorption maximum of the HV monocation radical at 560 nm under electrolysis. An ITO cell of the same type, but with no wiring, was used for the reference. Both were filled with the HV solution.

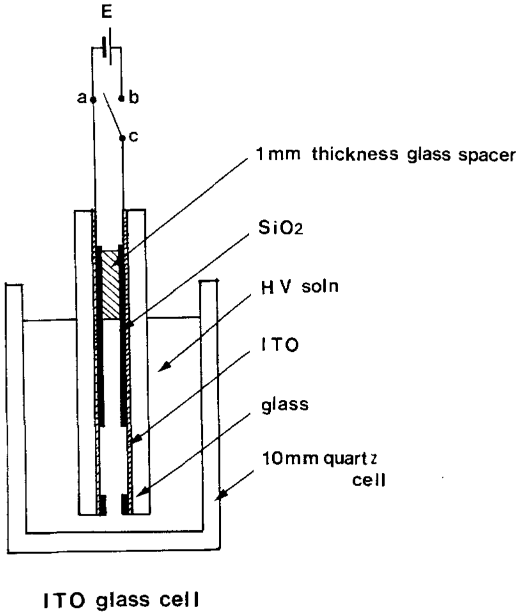

Fig. 1. The ITO glass cell. The electrode area is 0.95 cm^2.

Referring to Fig. 1, if *b* is connected with *c*, reduction of HV starts and the film of HV cation radicals begins to deposit on the ITO electrode. The quantity and the rate of formation of the HV cation radical can be determined by the change of the transmittance at 560 nm. After a few seconds' of electrolysis, the anode and the cathode are short circuited (*a*–*c*), so that erasure, i.e. the oxidation of HV cation radical takes place.

3. Results and discussion

3.1. *Voltammetry of HV*

The cyclic voltammograms of 0.01 mol dm^{-3} and 0.01 mol dm^{-3} $K_4Fe(CN)_6$ aqueous solutions are shown in Fig. 2. The platinum wire was used as the working electrode. The electrode potential was referred to the saturated silver–silver chloride electrode (SSCE). The ferrocyanide gave symmetrical reversible redox waves, while the separ-

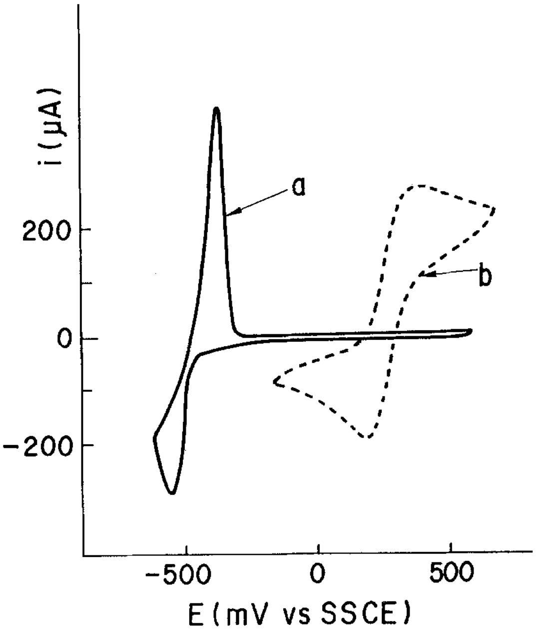

Fig. 2. Cyclic voltammograms of HV in aqueous solution (a) and $Fe(CN)_6^{4-}$ in aqueous solution (b) with Pt electrode, the surface area of which is 0.35 cm^2. Scan speed is 50 $mV s^{-1}$.

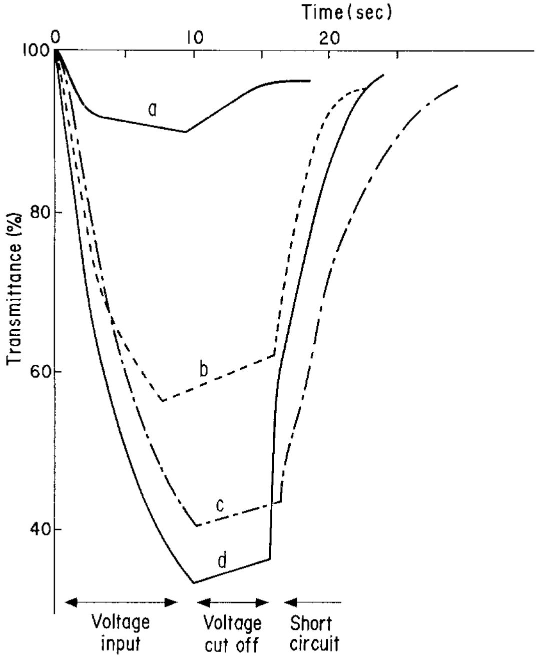

Fig. 3. Transparency–time characteristics of HV (a, b), HV–Fe(CN)$_6^{4-}$ (c) and HV–Fe(CN)$_6^{4-}$–NaH$_2$PO$_2$ (d) systems. Applied voltages are 1.7, 1.9, 0.7 and 0.7 V, respectively. 0.01 mol dm^{-3} HV, 0.01 mol dm^{-3} K$_4$Fe(CN)$_6$, 0.5 mol dm^{-3} NaH$_2$PO$_2$.

ated sharp reduction and oxidation waves of HV suggests the relatively strong adsorption of coloured HV monocation radical on the electrode.

The transparency vs time relations of 0.01 mol dm^{-3} HV aqueous solution under electrolysis are shown in Fig. 3. The transmittance was taken by the double beam monochrometer with the ITO cell (see Fig. 1).

Without addition of any Fe(CN)$_6^{4-}$ or NaH$_2$PO$_2$, the electrolyses of HV aqueous solution required an input voltage of 1.7–1.9 V (*a* and *b*) for the electrochromism and in this case the stability of the HV cation radical and the reliability in the repeated cycle with this system were not good, possibly due to the evolution of oxygen gas on the surface of the anode. If a non-gas evolving redox couple was added to the system, the reliability of the transmittance was improved. Thus an attempt was made to add Fe(CN)$_6^{4-}$ and NaH$_2$PO$_2$ to the HV aqueous solution. The transparency–time curves are shown by *c* and *d*, and these will be discussed later.

3.2. *Spectrophotometry of the HV–Fe(CN)$_6^{4-}$ and HV–Fe(CN)$_6^{4-}$–NaH$_2$PO$_2$ systems*

As Fig. 4 shows, HV aqueous solution has no absorption in the visible region, while the mixture of HV and Fe(CN)$_6^{4-}$ colours violet and the absorption maximum at 560 nm indicates the formation of HV monocation radicals. The spectra were taken with a 10 mm quartz cell. On further addition of NaH$_2$PO$_2$ the colour again fades. The transmittance at 560 nm is 43% without NaH$_2$PO$_2$ and 73% with the addition of 0.7 mol dm^{-3} NaH$_2$PO$_2$.

In the case of 0.015 mol dm^{-3} HV and 0.015 mol dm^{-3} Fe(CN)$_6^{4-}$ solution, the transmittance is 29% without the addition of NaH$_2$PO$_2$ and 50% with 0.7 mol dm^{-3} NaH$_2$PO$_2$. The transparency of the solution depends not only upon the concentration of NaH$_2$PO$_2$ but also upon those of HV and Fe(CN)$_6^{4-}$.

As shown in Fig. 2, the redox potentials of Fe(CN)$_6^{3-}$/Fe(CN)$_6^{4-}$ and HV differ to a large extent and it seems unlikely that Fe(CN)$_6^{4-}$ reduces HV directly, however, the fact that the HV–Fe(CN)$_6^{4-}$ mixture colours violet (λ_{max} = 560 nm) suggests that the redox potential of HV would be increased by Fe(CN)$_6^{4-}$ or the redox potential of Fe(CN)$_6^{4-}$ would be reduced by HV by formation of some adduct between them. The addition of NaH$_2$PO$_2$ to the HV–Fe(CN)$_6^{4-}$ system would lessen the above effects so that the transparency

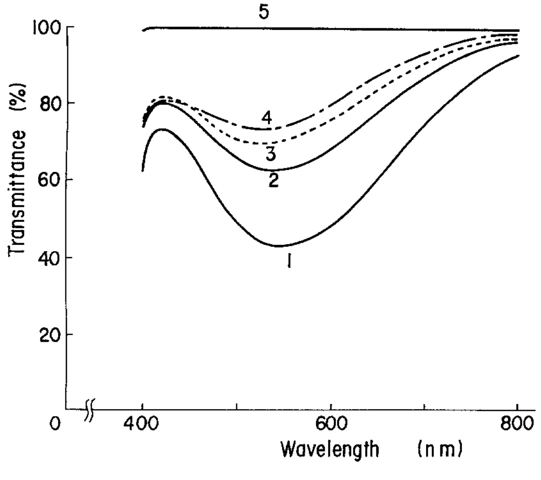

Fig. 4. Spectrophotometry of HV–Fe(CN)$_6^{4-}$ and HV–Fe(CN)$_6^{4-}$–NaH$_2$PO$_2$ system. 0.01 mol dm^{-3} HV; 0.01 mol dm^{-3} K$_4$Fe(CN)$_6$; NaH$_2$PO$_2$ 1 – 0 mol dm^{-3}, 2 – 0.2 mol dm^{-3}, 3 – 0.4 mol dm^{-3}, 4 – 0.7 mol dm^{-3}; 5 – 0.01 mol dm^{-3} aq. HV.

of the HV–$Fe(CN)_6^{4-}$–NaH_2PO_2 system would become higher than that without NaH_2PO_2.

Almost the same tendencies in spectra change were observed on addition of KBr to the HV–$Fe(CN)_6^{4-}$ mixture. The transmittance at 560 nm is 43% without KBr and more than 80% with the addition of 0.7 mol dm^{-3} KBr for the mixture of 0.01 mol dm^{-3} HV and 0.01 mol dm^{-3} $Fe(CN)_6^{4-}$. The effectiveness of making the HV–$Fe(CN)_6^{4-}$ system more transparent is larger with KBr than with NaH_2PO_2. Some other salts like KCl and KNO_3 also showed the same fading effects. These salt, strong electrolytes, would decompose the weakly formed HV–$Fe(CN)_6^{4-}$ adduct.

3.3. *Cyclic voltammetry of HV–$Fe(CN)_6^{4-}$ with and without NaH_2PO_2 or KBr*

A cyclic voltammogram of the HV–$Fe(CN)_6^{4-}$ system is shown in Fig. 5. Redox waves of $Fe(CN)_6^{4-}$ in the mixture, located at the right hand side, are different from the case without any other additives (see Fig. 2). The reduction peak current is far larger than that of oxidation and the mean redox potential in the mixture is about 100 mV more negative than that of the $Fe(CN)_6^{4-}$ aqueous solution. By the formation of some adduct, not yet identified, $Fe(CN)_6^{4-}$ is oxidized to some extent, resulting in the distortion of the symmetrical redox waves.

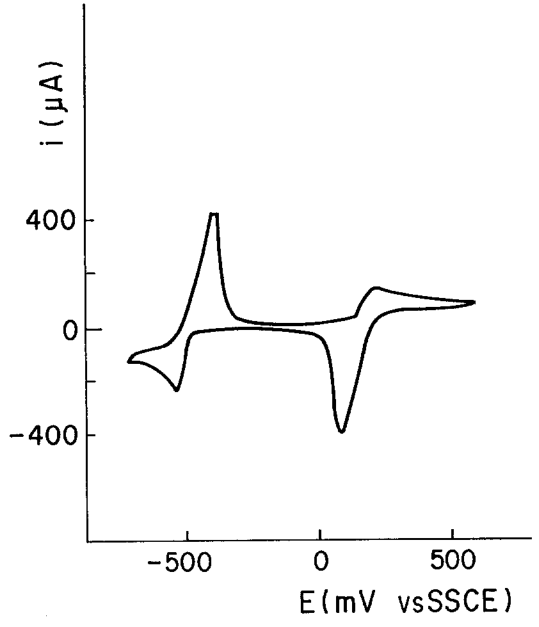

Fig. 5. Cyclic voltammogram of HV–$Fe(CN)_6^{4-}$ system with Pt electrode. Scan speed is 10 mV s^{-1}. 0.01 mol dm^{-3} HV, 0.01 mol dm^{-3} $Fe(CN)_6^{4-}$.

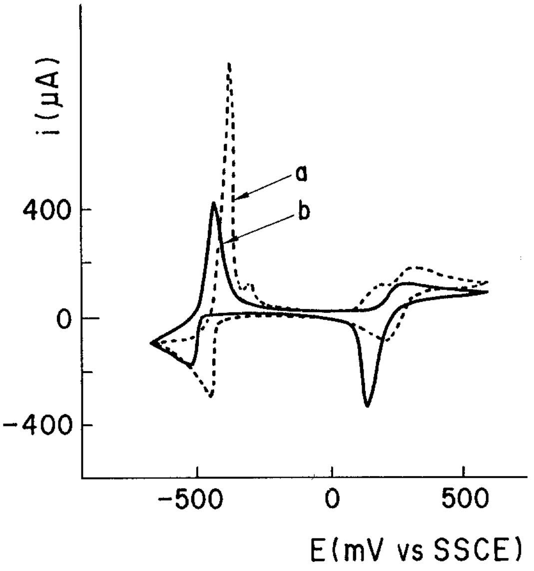

Fig. 6. Cyclic voltammograms of HV–$Fe(CN)_6^{4-}$–KBr system (a) and HV–$Fe(CN)_6^{4-}$–NaH_2PO_2 system (b) with Pt electrode. Scan speed is 10 mV s^{-1}. 0.01 mol dm^{-3}, 0.01 mol dm^{-3} $Fe(CN)_6^{4-}$, 0.5 mol dm^{-3} NaH_2PO_2 or KBr.

Fig. 6a shows the cyclic voltammogram of the HV–$Fe(CN)_6^{4-}$–KBr system. The redox waves observed in the lower potential region are attributable to the redox reaction of HV^{2+}/HV^{+}. The larger peak of the oxidation waves are attributable to the oxidation of the ordinary HV monocation radical, while the peak at the right hand is considered as the oxidation of $HV^{+\cdot}$ which adsorbs more strongly onto the electrode.

On the other hand, the redox waves observed in the higher potential region are due to the reaction $Fe(CN)_6^{3-}/Fe(CN)_6^{4-}$. During the cyclic voltammetries of HV–$Fe(CN)_6^{4-}$–KBr system, some violet residue appeared on the electrode, which did not disappear at the potential of the oxidation of $HV^{+\cdot}$. At the peak on the left hand side of the oxidation waves of $Fe(CN)_6^{4-}$, erasure of the HV 'residue' was observed.

On the other hand no such HV 'residue' was observed with the HV–$Fe(CN)_6^{4-}$–NaH_2PO_2 system in the cyclic voltammetry and the voltammogram gave no peak at the potential where the disappearance of the residue was observed with the HV–

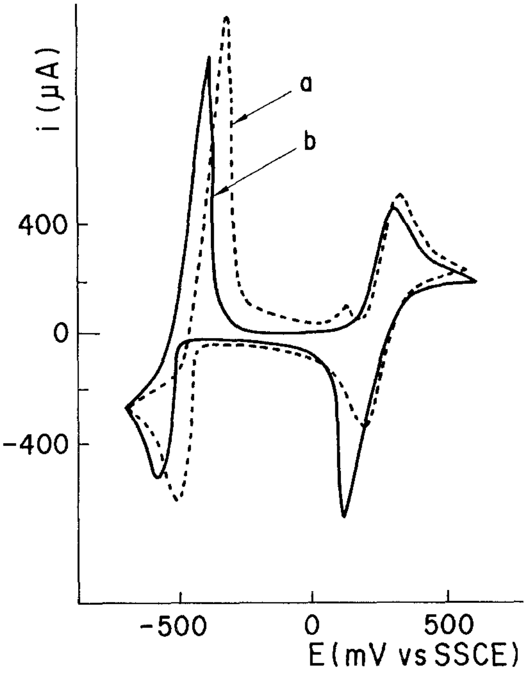

Fig. 7. Cyclic voltammograms of HV–Fe(CN)$_6^{4-}$–KBr system (a) and HV–Fe(CN)$_6^{4-}$–NaH$_2$PO$_2$ system (b) with ITO electrode. Scan speed is 10 mV s^{-1}. 0.01 mol dm^{-3} HV, 0.01 mol dm^{-3} Fe(CN)$_6^{4-}$, 0.5 mol dm^{-3} NaH$_2$PO$_2$ or KBr.

Fe(CN)$_6^{4-}$–KBr system. In the case of the KBr system, strongly adsorbed HV$^{+\cdot}$ accumulated on the electrode, while the PO$_2$ group of NaH$_2$PO$_2$ would interact with HV$^{+\cdot}$ preventing the formation of the residue.

The redox waves of HV and Fe(CN)$_6^{4-}$ taken with the ITO electrode are almost the same as those obtained with the Pt electrode shown in Fig. 5.

Fig. 7a shows the cyclic voltammogram of the HV–Fe(CN)$_6^{4-}$–KBr system with the ITO electrode as the working electrode. The peak at the right hand side oxidation wave of the HV oxidation waves was not observed with the ITO electrode, but the oxidation of the HV residue was also observed at the left hand side of the Fe(CN)$_6^{4-}$ oxidation wave.

Fig. 7b shows the cyclic voltammogram of the HV–Fe(CN)$_6^{4-}$–NaH$_2$PO$_2$ system. The peak at the right hand waves of the HV$^{+\cdot}$ oxidation was not detected in this system either. Furthermore the oxidation peak of the HV residue was not observed at all with the HV–Fe(CN)$_6^{4-}$–NaH$_2$PO$_2$ system using the ITO electrode. On the ITO electrode a small positive shift of the oxidation peak of Fe(CN)$_6^{4-}$ was observed and a deep and sharp reduction peak of Fe(CN)$_6^{3-}$. These factors suggest that Fe(CN)$_6^{4-}$ might be weakly adsorbed onto the electrode.

3.4. *Transparency–time characteristics of HV, HV–Fe(CN)$_6^{4-}$, HV–Fe(CN)$_6^{4-}$–NaH$_2$PO$_2$ system*

As shown in Fig. 3, the HV solution that has neither Fe(CN)$_6^{4-}$ nor NaH$_2$PO$_2$ needs ≈ 2 V for electrolysis and has little reproducibility in its electrochromism. The voltage seems to be too high for a practical electrochromic display. Addition of Fe(CN)$_6^{4-}$ to the HV solution should overcome the problem and when this was attempted the applied voltage became as low as 0.8 V. However, another problem appeared, namely the precipitation of the yellow residue on the display electrode. In contrast the HV–Fe(CN)$_6^{4-}$–NaH$_2$PO$_2$ system showed no residue in the voltammogram and was also reproducible both in erasure and colouring and had better response time than the systems without NaH$_2$PO$_2$ (Fig. 3a–c).

The response time, which depends upon each component of the HV–Fe(CN)$_6^{4-}$–NaH$_2$PO$_2$ system and the current density, is not sufficiently fast at the present time, but improvement of the response time will be reported in a subsequent paper.

4. Conclusion

Though there remain several problems with HV ECD, addition of Fe(CN)$_6^{4-}$ to the HV system has been shown to decrease the required applied voltage. Further addition of NaH$_2$PO$_2$ to the HV–Fe(CN)$_6^{4-}$ system improved the electrochromic effect on an ITO electrode in terms of both response time and the residue problem.

References

[1] J. Bruinink, C. G. A. Kregting and J. J. Ponjeé, *J. Electrochem. Soc.* **124** (1977) 1854.
[2] J. G. Fish and G. G. Barna, *ibid.* **128** (1981) 1290.
[3] H. T. van Dan and J. J. Ponjeé, *ibid.* **121** (1974) 1555.
[4] R. J. Jasinski, *ibid.* **124** (1977) 637.
[5] J. Bruinink and P. van Zanten, *ibid.* **124** (1977) 1232.
[6] R. C. Cieslinski and N. R. Armstrong, *ibid.* **127** (1980) 2605.